THEORETICAL STUDY OF CORRELATION IN TWO DIMENSIONAL HCP STRUCTURE

By

CHING-YUAN CHEN

Bachelor of Science

National Chung-Hsing University

Tai-Chung, Taiwan, R.O.C.

1973

Submitted to the Faculty of the Graduate College
of the Oklahoma State University
in partial fulfillment of the requirements
for the Degree of
MASTER OF SCIENCE
July, 1982

THEORETICAL STUDY OF CORRELATION IN TWO

DIMENSIONAL HCP STRUCTURE

Thesis Approved:

Bruce J. Anderson

Thesis Adviser

Jack J. Martin

Norman N. Durham

Dean of the Graduate College

PREFACE

This is a theoretical study of intensity cross correlation and forced Rayleigh scattering in a two dimensional system. Theoretical results are obtained for a simple rotational diffusion model and are evaluated numerically. The final results shed some insights into what may be expected in future experiments.

The author wishes to express his great appreciation to his principal adviser, Dr. B. J. Ackerson, for his guidance and patience throughout this study. Appreciation also is extended to my thesis committee members, Dr. E. E. Kohnke and Dr. J. J. Martin. The financial support from the Department of Physics, Oklahoma State University, of course made this thesis possible. Finally, the special thanks are expressed to my family, especially, to my 'FOREVER' father.

TABLE OF CONTENTS

LIST OF FIGURES

Figure Page

CHAPTER I

INTRODUCTION

It is well known that the particles in an isotropic system such as a liquid or gas are equally likely to be at any point $\vec{r}$ in space. However, if we consider two particles at a time, the presence of one particle at a point $\bar{r}_1$ limits the position $\bar{r}_2$ available to the other particle. Because there are particle interactions, different values of the relative position $\bar{r}_2-\bar{r}_1$ of any two particles in the system do not appear with equal likelihood. In other words, there exists a definite amount of correlation between the simultaneous positions $\bar{r}_2$ and $\bar{r}_1$ of the two particles.

The general configurational distribution function for all particles in the system is denoted by $F_N(\bar{r}_1,\bar{r}_2\cdots\bar{r}_N)$ and satisfies the normalization condition

$$\int_v F_N(\bar{r}_1,\bar{r}_2\cdots\bar{r}_N)d^3\bar{r}_1\ d^3\bar{r}_2\cdots d^3\bar{r}_N = 1 \qquad (1.1)$$

By integrating $F_N(\bar{r}_1,\bar{r}_2\cdots\bar{r}_N)$ over the coordinates $\bar{r}_2\cdots\bar{r}_N$ and multiplying the result by N, we obtain a single particle distribution function

$$F_1(\bar{r}_1) = N\int_v F_N(\bar{r}_1,\bar{r}_2\cdots\bar{r}_N)d^3\bar{r}_2\ d^3\bar{r}_3\cdots d^3\bar{r}_N \qquad (1.2)$$

where $F_1(\bar{r}_1)$ represents the particle density at the point $\bar{r}_1$. Obviously,

$\int_V F_1(\bar{r}_1)d^3r_1 = N$. The two-particle distribution function is defined as

$$F_2(\bar{r}_1,\bar{r}_2) = N(N-1)\int_V F_N(\bar{r}_1\cdots\bar{r}_N)d^3\bar{r}_3\cdots d^3\bar{r}_N = n^2 g^{(2)}(\bar{r}) \quad (1.3)$$

where $\bar{r} = \bar{r}_2 - \bar{r}_1$ and $g^{(2)}(\bar{r})$ is the pair distribution function of the system. In the case of noninteracting particles, $g^{(2)}(\bar{r}) = 1$. However, for real systems, $g^{(2)}(\bar{r})$ is generally different from 1. These distribution functions are of great importance because they may be related to macroscopic and thermodynamic properties of the material (1). For example, the density fluctuation θ is given by

$$\theta = 1 + n\int_A [g^{(2)}(\bar{r}) - 1]d^3\bar{r} \quad (1.4)$$

the compressibility κ_T by

$$\kappa_T = \frac{1}{nk_BT}\left[n\int_A [g^{(2)}(\bar{r}) - 1]d^3\bar{r} + 1\right] \quad (1.5)$$

the internal energy E by

$$E = \frac{3}{2}Nk_BT\left[1 + \frac{4\pi n}{3k_BT}\int_0^\infty u(\bar{r})g^{(2)}(\bar{r})r^2dr\right] \quad (1.6)$$

and the pressure P by

$$P = \frac{Nk_BT}{V}\left[1 - \frac{2\pi n}{3k_BT}\int_0^\infty \frac{\partial u(\bar{r})}{\partial r} g^{(2)}(\bar{r})r^3dr\right] \quad (1.7)$$

where n is the particle density in the system, $g^{(2)}(r)$ is the pair distribution function of the particles which is a function of $|\bar{r}|$ for fluids and which measures the probability of finding a pair of particles separated by a distance r and u(r) is the potential energy of interaction

between particles.

The pair correlation function $g^{(2)}(r)$ is also related to the intensity distribution $I(\bar{s})$ of radiation scattered by a sample,

$$I(\bar{s}) = I_o[1 + n \int_o^\infty [g^{(2)}(r) - 1] \frac{\sin(sr)}{sr} d^3r] \qquad (1.8)$$

where I_0 is the scattering from N isolated or noninteracting particles and $I(\bar{s})$ is a function of $|\bar{s}|$ for fluids. Here $\bar{s} = \bar{k}_s - \bar{k}_i$ is the difference between the scattered and the incident wavevectors, and the single particle form factor is taken to be unity. Thus, scattered intensity data of sufficient quality may be inverted numerically to determine $g^{(2)}(r)$ directly from experimental data.

$$g^{(2)}(r) = 1 + \frac{1}{2\pi^2 nr} \int_o^\infty [\frac{I(s)}{I_0} - 1]s \sin(sr)ds \qquad (1.9)$$

These fundamental relationships have led to much effort to measure $g^{(2)}(r)$ directly on one hand and to calculate $g^{(2)}(r)$ from $u(r)$ on the other. The theoretical work has been discussed and has taken many paths in many texts (1-7).

The early work of Prins and Petersen (8) is of interest because it is simple and qualitatively accurate. It treats a liquid as having a "local-solid" structure which becomes more random as the distance between particles increases. The model has potential for extension to higher order correlation functions as well. Furthermore, the recent work of Stillinger and Weber (9) also suggests hidden solid structure in fluids. To detect such structure would require the measurement of higher order correlation functions than $g^{(2)}(r)$, as the random ordering of an amorphous system on a large space or time scale averages this

information out of $g^{(2)}(r)$. These higher order correlation functions may be related to such important phenomena as freezing but have not been studied experimentally for pure fluids. However, there is currently experimental work being conducted on colloidal systems which may reveal such correlation functions.

The purpose of this thesis is to anticipate results for the measurement of higher order correlation functions from "two-dimensional" colloidal samples. While the formalism presented here applies strictly to a simple atomic fluid, it may also be applied to describe colloidal suspensions of highly interacting particles. Here the large colloidal particles are the "atoms" of the fluid and the solvent is the "vacuum" between particles. The pair correlation function describes the correlation between colloidal particles. The number fluctuations are those of the colloidal particles. The pressure is the osmotic pressure of the suspension.

For the local structure of a fluid we assume a two-dimensional hexagonal close packed structure which rotationally diffuses in time. The forced-Rayleigh and cross-correlation functions are computed for this system. These functions depend on $g^{(4)}(r)$, a four particle correlation function, in general. However, because we have a "local-solid" assumption, the correlation functions do not appear explicitly (in a way similar to Prins and Petersen). Functional forms are derived and they are evaluated numerically. New features are seen and discussed with respect to ordinary single detector equilibrium intensity autocorrelation.

CHAPTER II

THEORY

Light scattering has been studied for more than one hundred years. It has a broad range of applications in physics, chemistry, biology, polymer science and engineering. Here we only briefly mention the well known (21) relation between light scattering and correlation functions. Let us consider a plane wave incident on a single particle as shown in Figure 1.[10] Here $\bar{k}_I$ is the incident wave vector, $\bar{k}_s$ is the scattered wave vector, θ is the angle between the incident and scattered wave vector, ψ is the angle between the particle and the detector from the local origin, $\bar{r}_1$ is the vector between the origin and the particle, $\bar{r}_2$ is the vector between the origin and the detector, and $\bar{k}$ is the vector difference between the incident and scattered wave vector.

The electric field at the particle is

$$\bar{\varepsilon}_p = \bar{\varepsilon}_o \exp[i\bar{k}_I \cdot \bar{r}_1 - i\omega t] \tag{2.1}$$

and the scattered field at the detector is

$$\bar{\varepsilon}_s = \frac{\bar{\varepsilon}_p e^{i\bar{k}_s \cdot |\bar{r}_2 - \bar{r}_1|}}{|\bar{r}_2 - \bar{r}_1|} \tag{2.2}$$

If we assume $|\bar{r}_2| >> |\bar{r}_1|$ and $\frac{\bar{r}_2}{|\bar{r}_2|} = \frac{\bar{k}_s}{|\bar{k}_s|}$, then the electric field at the detector is

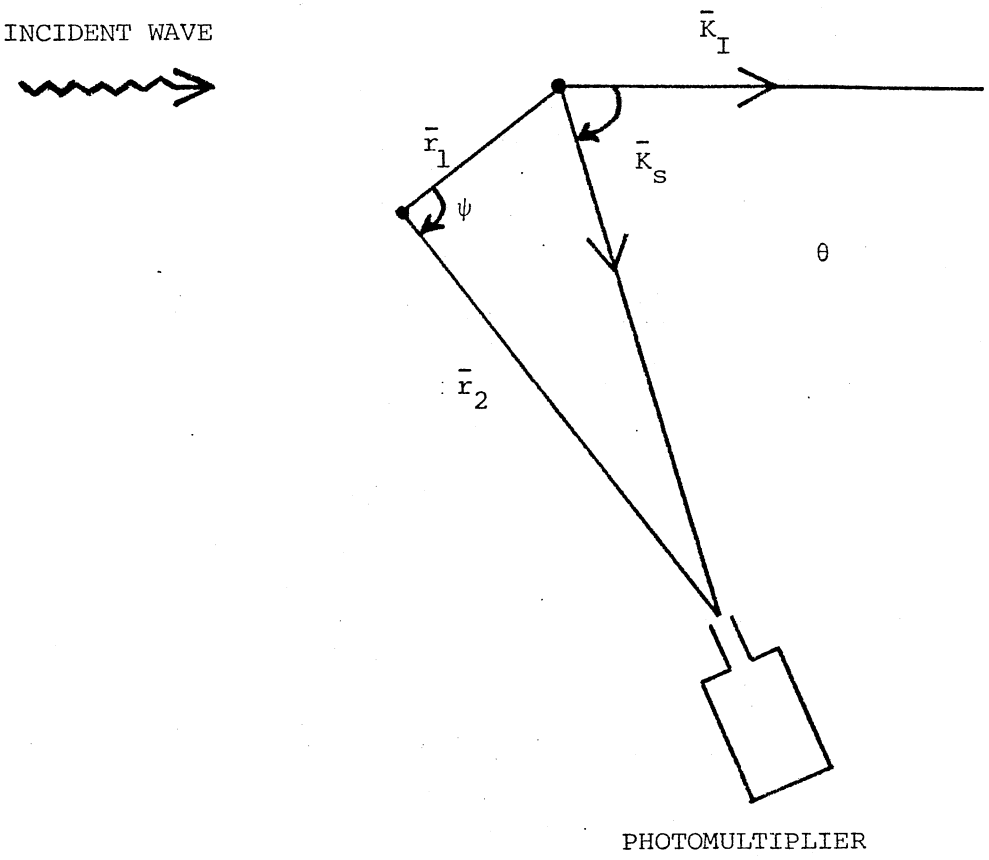

Figure 1. Light Scattering Geometry

$$\bar{\varepsilon}(r_2) = \bar{\varepsilon}_o e^{i\bar{k}_I\cdot\bar{r}_1 - i\omega t} \frac{1}{r_2} e^{ik_s(r_2 - \hat{r}_1\cdot\frac{\bar{r}_2}{|\bar{r}_2|})}$$

$$= \bar{\varepsilon}_o \frac{e^{ik_s r_2 - i\omega t}}{r_2} e^{i(\bar{k}_I - k_s\frac{\bar{r}_2}{|\bar{r}_2|})\cdot\bar{r}_1} \qquad (2.3)$$

By assuming the process is nearly elastic (i.e. $|\bar{k}_I| = |\bar{k}_s|$) then

$$\frac{\bar{r}_2}{|\bar{r}_2|} = \frac{\bar{k}_s}{|\bar{k}_s|}$$

$$\bar{k}_I - \bar{k}_s\frac{\bar{r}_2}{|\bar{r}_2|} = \bar{k}_I - \bar{k}_s = \bar{k}$$

$$|\bar{k}| = (k_I^2 + k_s^2 - 2k_I k_s\cos\theta)^{\frac{1}{2}} = 2k_I\sin(\tfrac{\theta}{2}) \qquad (2.4)$$

This is simply a Born approximation and the scattered field is

$$\bar{\varepsilon}(r_2) = [\bar{\varepsilon}_o \frac{e^{ik_s r_2 - i\omega t}}{r_2}]e^{i\bar{k}\cdot\bar{r}_1} \qquad (2.5)$$

When we consider scattering from N particles, the electric field correlation function becomes

$$\langle\bar{\varepsilon}(r_2,t)\bar{\varepsilon}^*(r_2,o)\rangle = \langle\sum_{i,j=1}^{N}\frac{\bar{\varepsilon}_o\bar{\varepsilon}_o^*}{r_2^2}e^{-i\omega t}e^{i\bar{k}\cdot(\bar{r}_i(t)-\bar{r}_j(o))}\rangle \qquad (2.6)$$

The high frequency term $e^{-i\omega t}$ will be canceled by a similar term,

when an intensity correlation function is formed. Thus we need only consider the correlation function

$$\langle \bar{\varepsilon}(t)\bar{\varepsilon}^*(o)\rangle = I_o \left\langle \frac{1}{N} \sum_{i,j=1}^{N} e^{i\bar{k}\cdot(\bar{r}_i(t)-\bar{r}_j(o))} \right\rangle$$

$$= I_o S(k,t) \tag{2.7}$$

where I_o is again the single scattering from N isolated or noninteracting particles and where

$$S(k,t) = \frac{1}{N} \sum_{i,j=1}^{N} \langle e^{i\bar{k}\cdot(\bar{r}_i(t)-\bar{r}_j(o))} \rangle \tag{2.8}$$

Since the photomultiplier can only measure the intensities, we must calculate $\langle I(t)I(o)\rangle = \langle \bar{\varepsilon}(t)\bar{\varepsilon}^*(t)\bar{\varepsilon}(o)\bar{\varepsilon}^*(o)\rangle$. If there are many scattering centers in the scattering volume, the probability distribution of $\bar{\varepsilon}(t)$ will be a Gaussian distribution and the correlation function is given by

$$\langle I(t)I(o)\rangle = I_o^2(|S(k,o)|^2 + \gamma|S(k,t)|^2) \tag{2.9}$$

where γ depends on geometrical factors and $\langle I(t)I(o)\rangle$ is called the autocorrelation function (11). It is a function averaged over time, relating the intensity at time zero to the intensity at time t. If not zero, it means that the value of intensity at time zero is related to the intensity at time t. As t increases, the autocorrelation must decrease and the autocorrelation approaches the square of the average intensity as $t \to \infty$. We can summarize some standard and well known properties of the autocorrelation function as follows (1):

1. The autocorrelation function depends on the time interval t_2-t_1

(in our case, $t_1 = 0$ and $t_2 = t$).

2. The quantity $\langle I(o)I(o)\rangle$ is identically equal to the mean square value of the variable I at time zero. In a stationary ensemble, it would be a constant and positive definite

$$\langle I(o)I(o)\rangle = \text{constant} > 0 \tag{2.10}$$

3. For any time interval t, the magnitude of $\langle I(o)I(t)\rangle$ can not exceed the value $\langle I(o)I(o)\rangle$.

4. The function $\langle I(t)I(o)\rangle$ is symmetric about $t = 0$.

5. As the time interval t becomes large, the values of I(o) and I(t) becomes uncorrelated and $\langle I(t)I(o)\rangle \rightarrow \langle I(o)\rangle^2$.

To realize these well known results experimentally one must use a large scattering volume such that Gaussian statistics prevails. In such a volume, there are many scattering centers, which may be independent particles or independent regions of correlated particles. Because each region is independent, the scattered field from each region is independent of the $\bar{\varepsilon}$-field from other regions. If there are a large number of these regions, there are a large number of contributions to the total scattered $\bar{\varepsilon}$-field. This is similar to a random walk of E-fields which tends towards a Gaussian distribution. The important point is that a Gaussian distribution of scattered $\bar{\varepsilon}$—fields can be completely characterized by $g^{(2)}(r,t)$ a time dependent two-particle correlation function similar to the time independent $g^{(2)}(r)$ shown in Equation (1.9). We wish to explore the newer techniques of forced Rayleigh and cross correlation scattering to investigate microscopic liquid order. To examine higher order correlation functions, however, requires a violation of Gaussian statistics, which is accomplished by looking at only one or a few corre-

lation regions. On this scale we expect that the fluid will have nearly a solid-like order as assumed in the Prins and Petersen model.

In our model we assume that the scattering volume is so small that only a single crystal structure is in it at any time. The sample is assumed to be fairly incompressible so that number fluctuations are small. Only rotations of the lattice and not vibrations will be considered in intensity fluctuation.

For stimulated Rayleigh scattering the crystal correlation region will be oriented by crossed laser beams. Subsequent decay of the orientation of the crystal correlation region is monitored by a probe beam. The scattered intensity measured by the probe beam is similar to previous intensity calculation and is given by

$$\langle I(k) \rangle = \sum_{\ell,m} \int \varepsilon_o^2 e^{-\alpha(r_\ell^2+r_m^2)} e^{i\bar{k}\cdot(\bar{r}_\ell-\bar{r}_m)} P\{r\}\cdots \qquad (2.11)$$

The cross correlation function for the scattered intensity into two separate detectors, described by the scattered wavevectors $\bar{k}$ and $\bar{q}$, is given by

$$\langle I(k,q) \rangle = \sum_{\ell,m,n,p} \int \varepsilon_o^4 e^{-\alpha(r_\ell^2+r_m^2+r_n^2+r_p^2)} e^{i\bar{k}\cdot(\bar{r}_\ell-\bar{r}_m)} \times e^{i\bar{q}\cdot(\bar{r}_n-\bar{r}_p)} P\{\bar{r}\}\cdots \qquad (2.12)$$

where P is the probability for finding the particles at positions {r} as a function of time. The factor $e^{-\alpha r^2}$ in expressions (6) and (7) accounts for the scattering volume size and α is set at unity in MKS units. The sums ℓ, m, n, p run over the lattice sites.

By expanding $e^{i\bar{k}\cdot(\bar{r}_\ell-\bar{r}_m)}$ and $e^{i\bar{q}\cdot(\bar{r}_n-\bar{r}_p)}$ into Bessel's expansions (12), the correlation functions become

$$\langle I(k)\rangle = \varepsilon_o^2 \int \left[\sum_{\ell,m} e^{-\alpha(r_\ell^2+r_m^2)} \sum_s i^s J_s(k_{ll}|\bar{r}_\ell-\bar{r}_m|) e^{is(\theta_{\ell m}+\theta)}\right] x\ P(\psi,\psi_o) \tag{2.13}$$

$$\langle I(k,q)\rangle = \varepsilon_o^4 \int \left[\sum_{\ell,m} e^{-\alpha(r_\ell^2+r_m^2)} \sum_s i^s J_s(k_{ll}|\bar{r}_\ell-\bar{r}_m|) e^{is(\theta_{\ell m}+\theta)}\right] x\ P(\psi,\psi_o)$$

$$x \left[\sum_{n,p} e^{-\alpha(r_n^2+r_p^2)} \sum_t i^t J_t(q_{ll}|\bar{r}_n-\bar{r}_p|) e^{it(\theta_{np}+\phi)}\right] \tag{2.14}$$

To simplify calculations and yet retain some physical reality in the model, we consider the particles to be in fixed lattice positions and to move only as a rotation of the whole unit (at least in the scattering volume). Thus the probability P for finding the particles in a certain position is much easier to describe than the general case. The particles each occupy a site in a lattice and the orientation of the lattice at time t with respect to a fixed Z-axis is determined by ψ, with ψ_o for t = 0. These angles are shown in Figure 2. The $\bar{k}$ direction is associated with t = 0, and θ gives the "lattice" orientation with respect to this direction. The angle $\theta_{\ell m}$ references particles to one another in the plane. Similarly for $\bar{q}_{ll}$ the lattice orientation is described by ϕ. For a two-dimensional system we have taken the projection of $\bar{k}$ and $\bar{q}$ along the plane to find $\bar{k}_{ll}$ and q_{ll}, respectively. These vectors describe the scattering.

For convenience we further simplify notation as follows:

$$\langle I(k,q)\rangle = \varepsilon_o^4 \int \sum_{s,t} A_s(k) A_t(q) e^{is(\psi_o-\eta)} e^{it(\psi-\xi)} P(\psi,\psi_o)\, d\psi\, d\psi_o$$

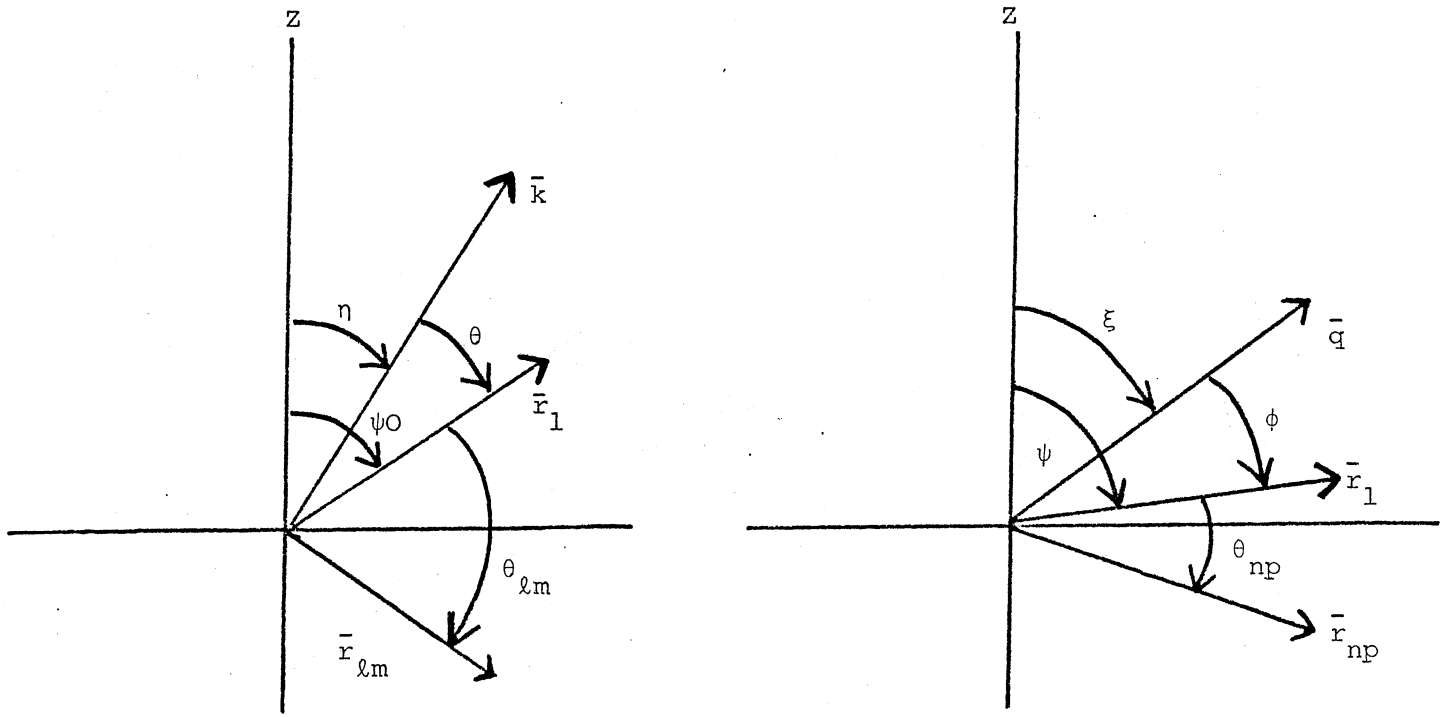

Figure 2. Particle and Detector Projection Onto Sample Plane

$$\langle I(k)\rangle = \varepsilon_o^2 \int \sum_s A_s(k) e^{is(\psi_o-\eta)} P(\psi,\psi_o)\, d\psi d\psi_o \tag{2.15}$$

where

$$A_s(k) = \sum_{\ell,m} e^{-\alpha(r_\ell^2+r_m^2)} J_s(k_{ll}|\bar{r}_\ell-\bar{r}_m|) i^s e^{is\theta_{\ell m}}$$

$$A_t(q) = \sum_{n,p} e^{-\alpha(r_n^2+r_p^2)} J_t(q_{ll}|\bar{r}_n-\bar{r}_p|) i^t e^{it\theta_{np}} \tag{2.16}$$

Now we suppose that $P(\psi,\psi_o)$ obeys a rotational diffusion dynamics such that

$$\frac{\partial P(\psi,\psi_o)}{\partial t} = D \frac{\partial^2 P(\psi,\psi_o)}{\partial \psi^2}, \quad 0 \le \psi \le 2\pi \tag{2.17}$$

where D is a phenomenological rotational diffusion constant.

We assume a power series expansion for $P(\psi,\psi_o)$ such that

$$P(\psi,\psi_o) = \sum_m E_m e^{im\psi} \tag{2.18}$$

If P is real, we have to sum from -m to m with $E_m = E_{-m}$. By substituting $P(\psi,\psi_o)$ into $\frac{\partial P}{\partial t}$ and $\frac{\partial^2 P}{\partial \psi^2}$ we have

$$\frac{\partial P(\psi,\psi_o)}{\partial t} = \sum_m \frac{\partial E_m}{\partial t} e^{im\psi}$$

$$D \frac{\partial^2 P(\psi,\psi_o)}{\partial \psi^2} = \sum_m DE_m(-m^2) e^{im\psi} \tag{2.19}$$

thus

$$\frac{\partial E_m}{\partial t} = -m^2 D E_m \tag{2.20}$$

This is easily solved to find

$$E_m = E_{mo} e^{-m^2 Dt} \tag{2.21}$$

Since the lattice has some given position at t = 0, the initial value is given by Green's function condition

$$P(t=0) = \delta(\psi-\psi_o) = \sum_m E_{mo} e^{im\psi} \tag{2.22}$$

By imposing $e^{-in\psi}$ on both sides and integrating, we find

$$\int e^{-in\psi}\, \delta(\psi-\psi_o)\, d\psi = \sum_m E_{mo} \int e^{i(m-n)\psi} d\psi$$

The left side immediately gives $e^{-in\psi_o}$ and the right side gives

$$\sum_m E_{mo} \int e^{i(m-n)\psi} d\psi = 2\pi \sum_m E_{mo} \left(\frac{1}{2\pi}\right) \int e^{i(m-n)\psi} d\psi$$

$$= 2\pi \sum_m E_{mo}\, \delta_{mn}$$

$$= 2\pi E_{no}$$

Thus

$$e^{in\psi_o} = 2\pi E_{no}$$

Since

$$E_m = E_{mo}\, e^{-m^2 Dt}, \tag{2.23}$$

then the Green function is

$$P(\psi,\psi_o) = \sum_m \frac{1}{2\pi} e^{im\psi_o} e^{im\psi} e^{-m^2 Dt} \tag{2.24}$$

The averaged scattered intensity for the cross correlation for two detectors is given in equilibrium by averaging over a uniform distribution of initial states for ψ_o to find

$$\langle I(k,q)\rangle = 2\pi \sum_m A_m(k) A_{-m}(q) e^{-im(\eta-\xi)} e^{-m^2 Dt} \tag{2.25}$$

The "forced-Rayleigh" signal is produced by the selected initial orientation ψ_o and found by averaging over ψ for subsequent times.

$$\langle I(k)\rangle = \sum_m A_m(k) e^{im(\eta-\psi_o)} e^{-m^2 Dt} \tag{2.26}$$

From the $e^{-m^2 Dt}$ term we see that higher order harmonics of $(\xi-\eta)$ or $(\eta-\psi_o)$ decay more rapidly in time. In some sense the cross correlation result is the "square" of the forced Rayleigh result. Both results depend on a relative measurement of angle $(\xi-\eta)$ or $(\eta-\psi_o)$. For forced Rayleigh scattering the initial position is physically prepared, while for cross correlation it is a fluctuation at $I(\bar{k}, t=0)$ which triggers the subsequent measurement at $I(\bar{q},t)$.

In the next sections we calculate some typical correlation functions and discuss their significance.

CHAPTER III

COMPUTATION

The evaluation of the $A_m(k)$ terms and subsequently the cross correlation and forced Rayleigh scattering functions are computed numerically. This is done for a two dimensional model because the first experiments will be done in this reduced dimension. The reason for this is that a two dimensional structure produces a scattering pattern in k-space which is more easily detected. A three dimensional structure produces reciprocal lattice points while a two dimensional structure produces reciprocal lines. It is easier to position detectors to intersect lines than points. The possible orientations are also reduced in two dimensions which means that stronger intensity correlations can be measured. In this case there is less "space" to average the k-space structure over resulting in less smearing out of the k-space structure.

For our two dimensional lattice we take a two-dimensional HCP structure as shown in Figure 3. For the 19 particles shown in the figure there are 171 pairs to be considered in the computation of $A_m(k)$. Clearly a computer is a great help in such an evaluation. The difficult part of this calculation is accurate estimation of $J_n(x)$. Both the order n and the argument x change and we must find a good recurrence relations for the cases : $n \geq x$ and $n < x$. For $n \geq x$, it is not difficult for us to get good numerical estimates of $J_0(x)$ and $J_1(x)$. From these two leading terms, the higher order terms can be calculated very

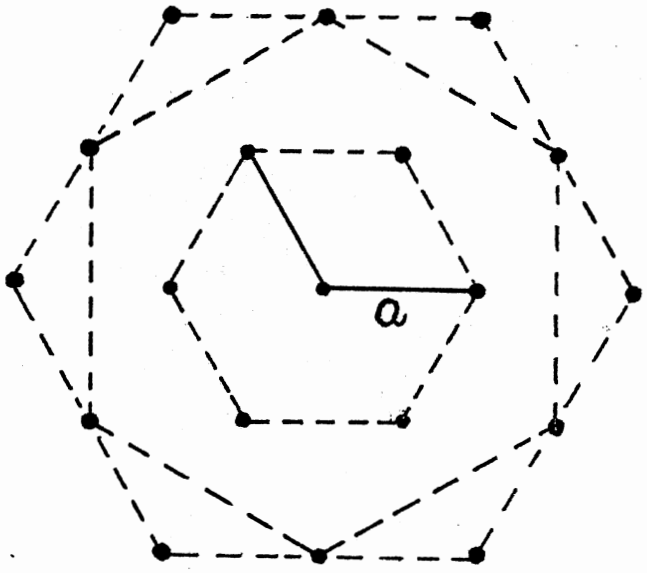

Figure 3. Hexagonal Close-Packed Structure Used in This Two Dimensional Study

accurately without much significant error using the recurrence relation for Bessel functions. However, we have a difficulty once the argument becomes larger than the order. A different recurrence relation has been found and fitted. A careful check has been made of this procedure, since we do not want any discrepancy from the limited values that can be found in tables. Any small error can cause a great error as it propagates through many iterations in the calculation.

We discuss both cases separately as follows:

(I) $n \geq x$ (i.e. the order greater than the argument).

Let us introduce a generating function $G(x,t) = e^{(x/2)(t-1/t)}$ and expand this generating function in a Laurent's series. We obtain

$$e^{(x/2)(t-1/t)} = \sum_{n=-\infty}^{\infty} J_n(x) t^n \tag{3.1}$$

Simply by differentiating the generating function partially with respect to t, substituting Equation (3.1) for the exponential and equating the coefficients of the same powers of t, we obtain

$$J_{n-1}(x) + J_{n+1}(x) = \frac{2n}{x} J_n(x) \tag{3.2}$$

This is a three-term recurrence relation. By finding accurate values for $J_0(x)$ and $J_1(x)$, any higher order terms will be found from this equation. The numerical approximations of $J_0(x)$ and $J_1(x)$ shown below were used to generate higher order J_n's.

$$\begin{aligned} J_0(x) &= FO*COS(GO)/\sqrt{x} \\ J_1(x) &= F1*COS(G1)/\sqrt{x} \end{aligned} \tag{3.3}$$

where the * indicates multiplication and where

$$
\begin{aligned}
FO &= 0.79785-0.00000077*x-0.0055274*x^2-0.00009512*x^3 \\
&\quad + 0.00137237*x^4-0.00072805*x^5+0.00014476*x^6 \\
GO &= x-0.7854-0.041664*x-0.00003954*x^2+0.0026257*x^3 \\
&\quad - 0.00054125*x^4-0.00029333*x^5+0.00013558*x^6 \qquad (3.4) \\
F1 &= 0.79788+0.00000156*x+0.016597*x^2+0.00017105*x^3 \\
&\quad - 0.0024951*x^4+0.0011365*x^5-0.00020033*x^6 \\
G1 &= x-2.3562+0.12499*x+0.0000565*x^2-0.0063788*x^3 \\
&\quad + 0.00074348*x^4+0.00079824*x^5-0.00029166*x^6
\end{aligned}
$$

Accurate values for the J_n's were obtained numerically by this technique. The leading terms $J_0(x)$ and $J_1(x)$ can also be found from tables (12-15).

(II) $n < x$.

The recurrence relation in Part (I) does not work accurately for this case. Here we have to work down from higher order terms by assuming this higher order is much higher than the order we wish to obtain. Because there are restrictions on the range of numbers that the computer can manipulate, we have to choose a number for this order which is sufficiently high without pushing the limitations of the computer. For example, we choose a value of n such that we can set

$$J_{n+1}(x) = 0 \qquad (3.5)$$

and

$$J_n(x) = C \qquad (3.6)$$

where C is a small constant number. By using

$$J_{n-1}(x) = \frac{2n}{x} J_n(x) - J_{n+1}(x) , \tag{3.7}$$

$J_{n-1}(x)$, $J_{n-2}(x)$.....etc. can be computed. Since C is arbitrary, the J_n's are all off by a common factor. This factor is determined by the condition

$$J_o(x) + 2 \sum_{m=1}^{\infty} J_{2m}(x) = C \tag{3.8}$$

Solving for C and rescaling $J_{n-1}(x)$, $J_{n-2}(x)$.....etc. ultimately generates whatever term we wish to calculate. The accuracy of this calculation can be checked by trying a different value for n than we chose initially. In our calculation, we use an order which is always 20 larger than the order we wish to calculate. The order was chosen to be no more than 20 larger than the order we want, because there is a limit on the largest, 10^{38}, and the smallest, 10^{-38}, numbers which the PDP 11 digital computer can handle.

Now, we can calculate $A_n(k)$, the coefficients in the average intensity cross correlation. We have complex values in general

$$A_n(k) = \sum_{\ell,m} e^{-\alpha(r_\ell^2+r_m^2)} i^n J_n(k_{11}|\bar{r}_\ell-\bar{r}_m|) e^{in\theta_{\ell m}} \tag{3.9}$$

which must be separated into real and imaginary parts for computation as follows

$$A_n(k) = RE(A_n(k)) + iIM(A_n(k)) \tag{3.10}$$

This computation showed good agreement with selected values picked from

tables (12,15).

Next we must calculate k_{11} and q_{11}. This is facilitated by considering the projection of the scattered wavevector k onto the sample plane as shown in Figure 4.

As mentioned earlier, we have

$$|\bar{k}| = |\bar{k}_s - \bar{k}_I| = \frac{4\pi n}{\lambda} \sin(\frac{\theta}{2}) \tag{3.11}$$

Since the path difference for the first constructive interference is

$$S \sin(\theta) = \lambda$$

we have

$$\theta = \sin^{-1}(\frac{\lambda}{S}) \tag{3.12}$$

and the separation between Bragg's planes is

$$S = a \cos(\theta) \tag{3.13}$$

where a is the lattice constant (a = 1.2 um in our calculation) and λ is incident wavelength (λ = 0.6328 um). From above known values, we can find the angle between the vector $\vec{k}$ and the sample plane. Then the projected k_{11} which probes the structure is:

$$k_{11} = |\bar{k}| \cos(\beta) = \frac{4\pi n}{\lambda} \cos(\frac{\theta}{2}) \sin(\frac{\theta}{2}) = \frac{2\pi n}{\lambda} \sin(\theta) \tag{3.14}$$

After we find the projection of $\bar{k}$ on the sample plane, the angle $\theta_{\ell m}$ must be computed. To do this we use the solid state basis vectors for the two-dimensional hexagonal structure.

From Figure 5, we can assign the coordinates for particle m, (the

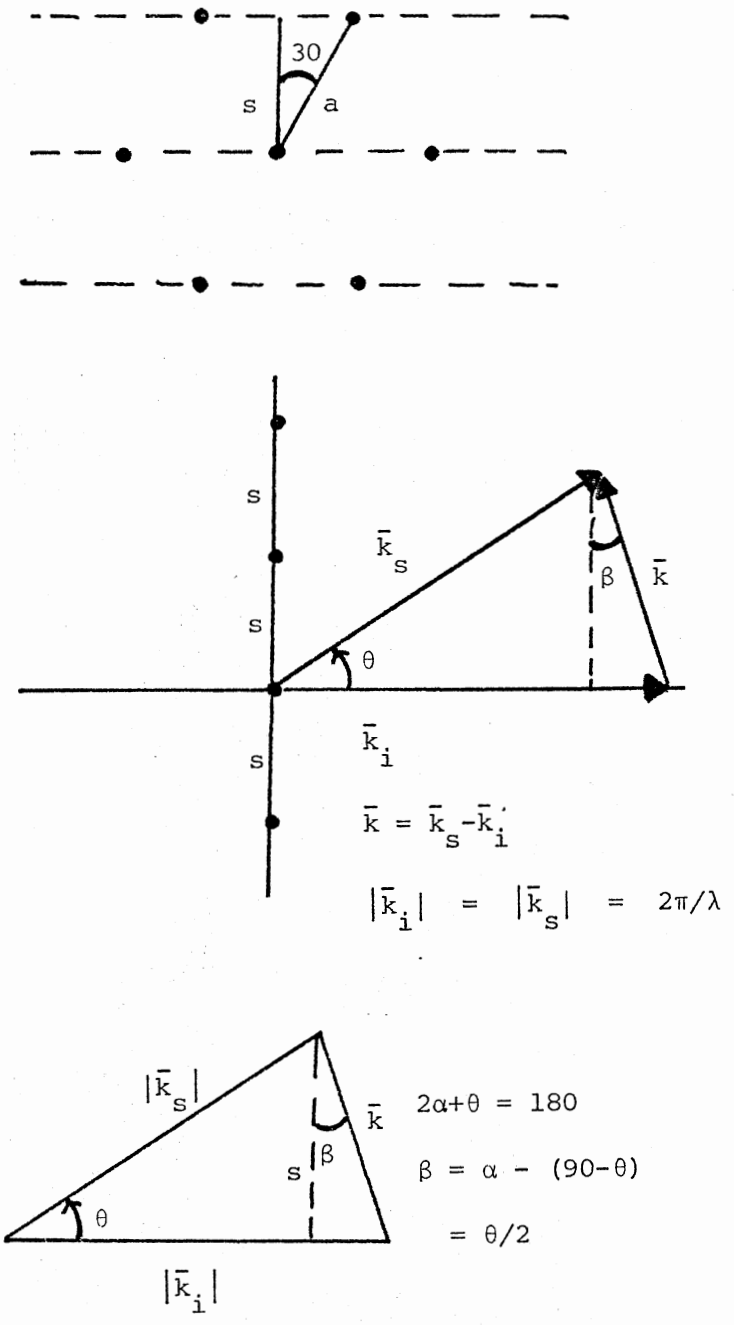

Figure 4. Calculation of the Projection of k on the Sample Plane

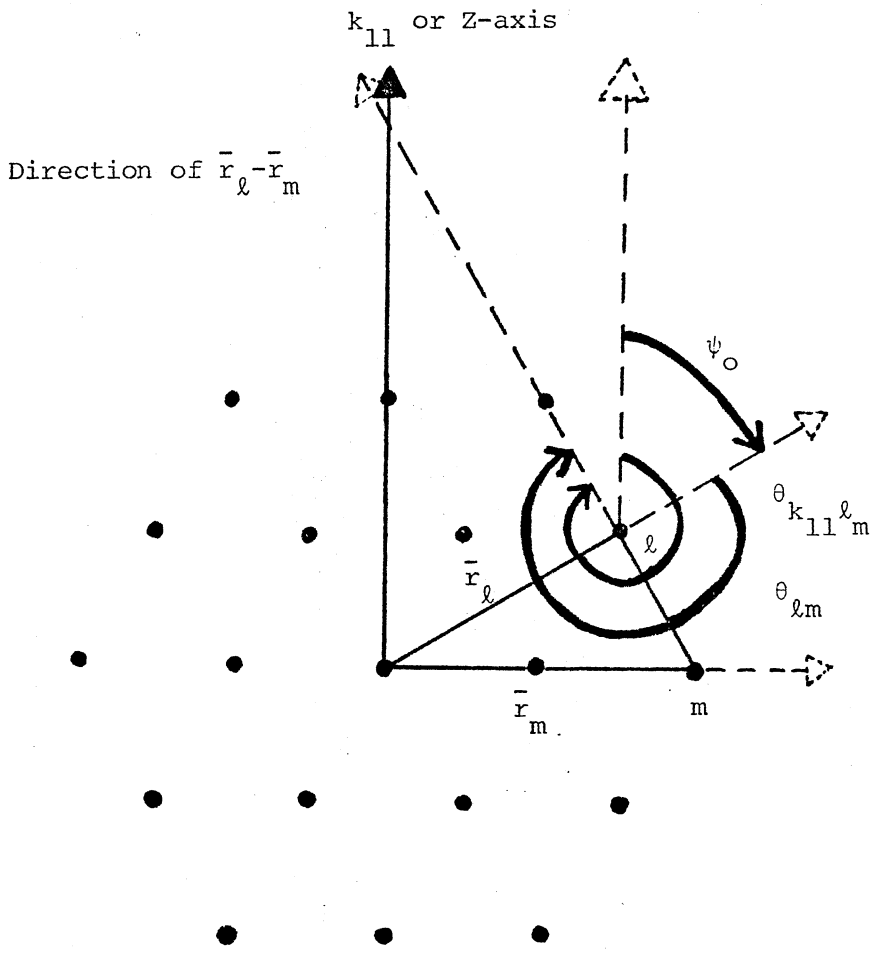

Figure 5. Relation Between Angles $\theta_{\ell m}$, $\theta_{k_{ll}\ell m}$ and ψ_o

variable particle, labeled by (P,Q)) and particle 1, (the fixed particle, labeled by (M,N)). Here P, Q, M, N are integer variables. The vertical and horizontal components for the particle's position are expressed by V1(M,N) and V2(M,N), respectively. Explicitly for an HCP structure we have

$$V1(M,N) = (M-2N)a/2$$

and (3.15)

$$V2(M,N) = \sqrt{3}\,Ma/2$$

where a again is the lattice constant.

When we expand $e^{ik_{11}|\bar{r}_1-\bar{r}_m|\cos(\theta_{k_{11}\ell m})}$ into a Bessel's function series, we have $\theta_{k_{11}\ell m}$ between k_{11} and the difference of $\bar{r}_1-\bar{r}_m$. The direction of vectors and angles have to be carefully determined. From the Figure 2 in Chapter II, we can see $\theta = \psi_o$ when k_{11} is on the z-axis and

$$\theta_{\ell m} + \theta = \Theta_{\ell m} + \psi_o = \theta_{k_{11}\ell m} \tag{3.16}$$

so $$\theta_{\ell m} = \theta_{k_{11}\ell m} - \psi_o$$

In the computer program, Q1 and QO correspond to $\theta_{k_{11}\ell m}$ and ψ_o, respectively. Further details may be found in the program given in Appendix II (statements 110 to 422).

By combining all the terms in $A_n(k)$, we obtain $A_1(k)$, $A_2(k)$....$A_n(k)$ separately and store them for further computation. Once we have these coefficients in the computer storage, time-independent and time-dependent correlations can be computed immediately. The averaged intensity of the

scattered light and its correlations are given in Equation (2.25) and (2.26). Here we will only present the normalized cross correlation function as follows:

$$Q(k,\underline{q}) = \frac{\langle I(k,\underline{q})\rangle}{\langle I(k)\rangle\langle I(q)\rangle} = \frac{\langle I(k,\underline{q})\rangle}{\langle I(k)\rangle^2} \qquad (3.17)$$

where $\xi-\eta$ is the angle between the projections of wavevectors k and q on the sample plane. Furthermore, k and q are taken to have the same magnitude, a value which corresponds to position of the first Debye-Scherrer ring. We only have to change $\xi-\eta$ from 0 to 180° to get the corresponding intensities. For convenience, we can fix one wavevector projection on z-axis and rotate the other from 0 to 180°. All the $A_n(k)$ and the computer program are given in the Appendix II.

CHAPTER IV

RESULTS AND DISCUSSION

For our results, we present two cases. One is cross correlation from two detectors and the other is the autocorrelation for forced-Rayleigh scattering. For each case, we will present three sets of figures.

1. The time-independent correlation as a function of angles.

2. The time-dependent correlation as a function of angles for several different times.

3. The time-dependent correlation for fixed angles.

4. In the final two figures, we will present the anti-correlation in the cross correlation case and comparison between correlation and anti-correlation.

Figure 6 gives the relation between cross correlation and the detector separation angle (ξ-η). In a simple hexagonal crystal structure, we have a six-fold scattered intensity pattern for the diffraction pattern. Because of the underlying symmetry, we get maximum intensity correlation when one detector is at $\xi = 0^{\circ}$ and the other detector at $\eta = 60^{\circ}$, 120° ... etc. By the same argument we have anti-correlation when one detector is maximum at $\xi = 0$, the other detector is dark at $\eta = 30^{\circ}$, 90°, 150° ... etc. Due to the finite scattering volume, diffraction gives finite light scattering intensities to both detectors and the correlation does not go to zero anywhere. For single detector equilibrium autocorrelation, there is no angle dependence

because the initial orientation is averaged over all angles in equilibrium. However, for a sample initially prepared by crossed beams in a forced Rayleigh scattering experiment, we see the decay from the initial structure shown in the Figure 7.

Figure 8 shows the decrease in the amplitude of the cross correlation function when time-dependence is considered. Figure 9 shows the corresponding decay of the forced-Rayleigh scattered intensity. As the decay time in the correlation functions increases, the correlation function magnitudes changes. Not only do we have a monotonic decrease in the correlation functions, but there are also angles (e.g. 30°) when we have anti-correlations, where the correlation function increases. This comparison has been given in Figures 8-9 for Dt = 0, 0.001 and 0.01.

Figure 10 displays a time-dependent graph for a fixed angle. It shows that the cross correlation function decays very fast as time increases. This can also be seen from equation where the term $\exp(-m^2 Dt)$ strongly controls the cross correlation function to give this fast exponential decay.

In this thesis we have seen that a local solid assumption for fluid structure can lead to forced Rayleigh and cross correlation experimental results which are quite different from the usual single detector autocorrelation experiment from fluid systems. Angular structure in the scattered intensity is related to the symmetry of the local particle structure. If we had a square lattice structure, we should correlate maximally at $\xi-\eta = 0^{\circ}$, 90°, and 180° rather than at $\xi-\eta = 0^{\circ}$, 60°, 120°, and 180° as for the HCP lattice. Thus, such experiments should reveal local symmetry or lack of it. Variation of the scattering volume combined with correlation should reveal structural correlation lengths.

The unusual phenomena of anti-correlation is predicted and should be observed experimentally. Finally, while the calculations are quite involved, it seems that the basic static and dynamic features are reproduced fairly well by the low mode (n=6) having the symmetry of the lattice. This may be a great help in modeling results of future experiments.

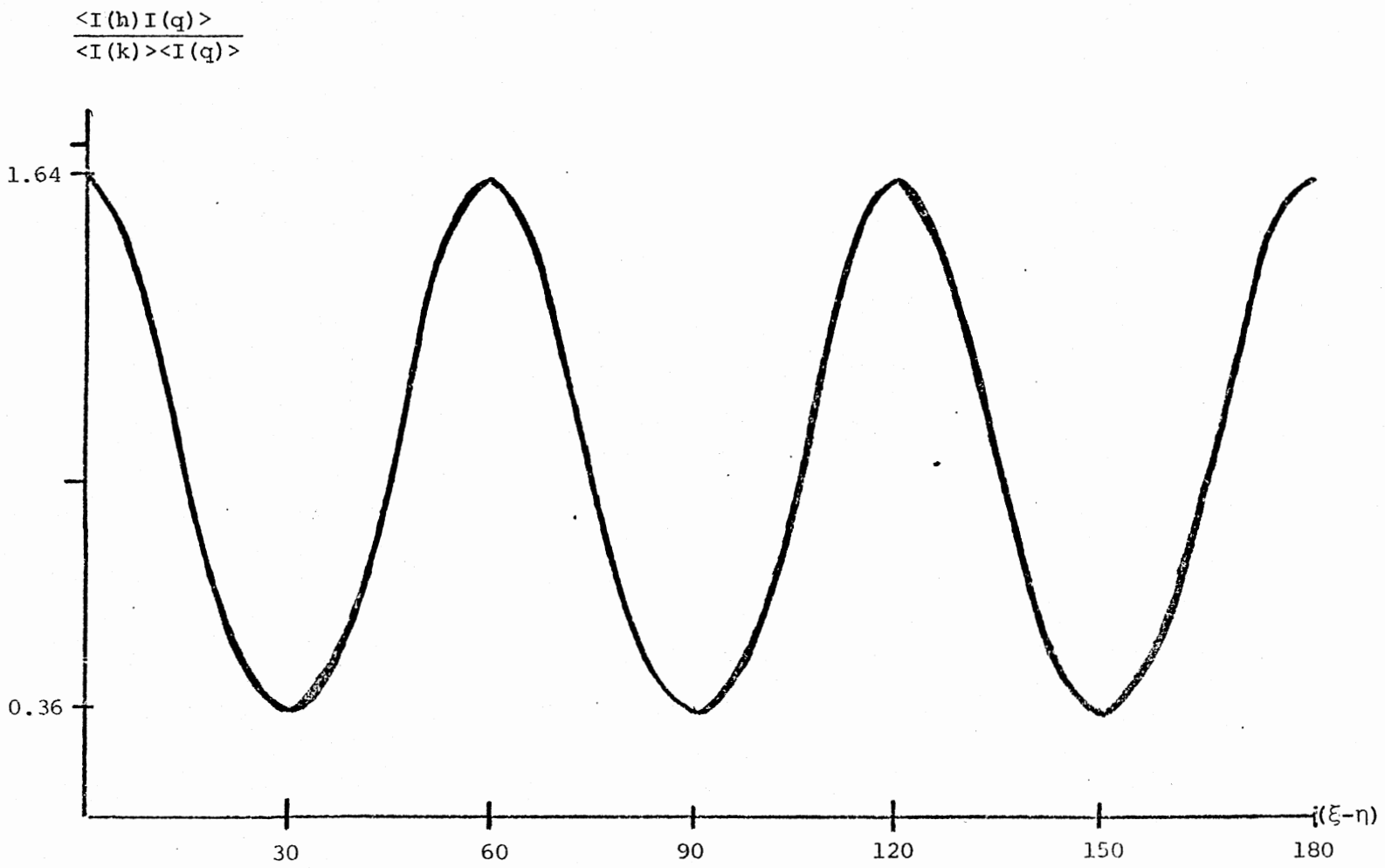

Figure 6. Time-independent Cross Correlation as a Function of the Angle (ξ-η). The Cross Correlation Has Maximum at Angles 0, 60, 120 and 180

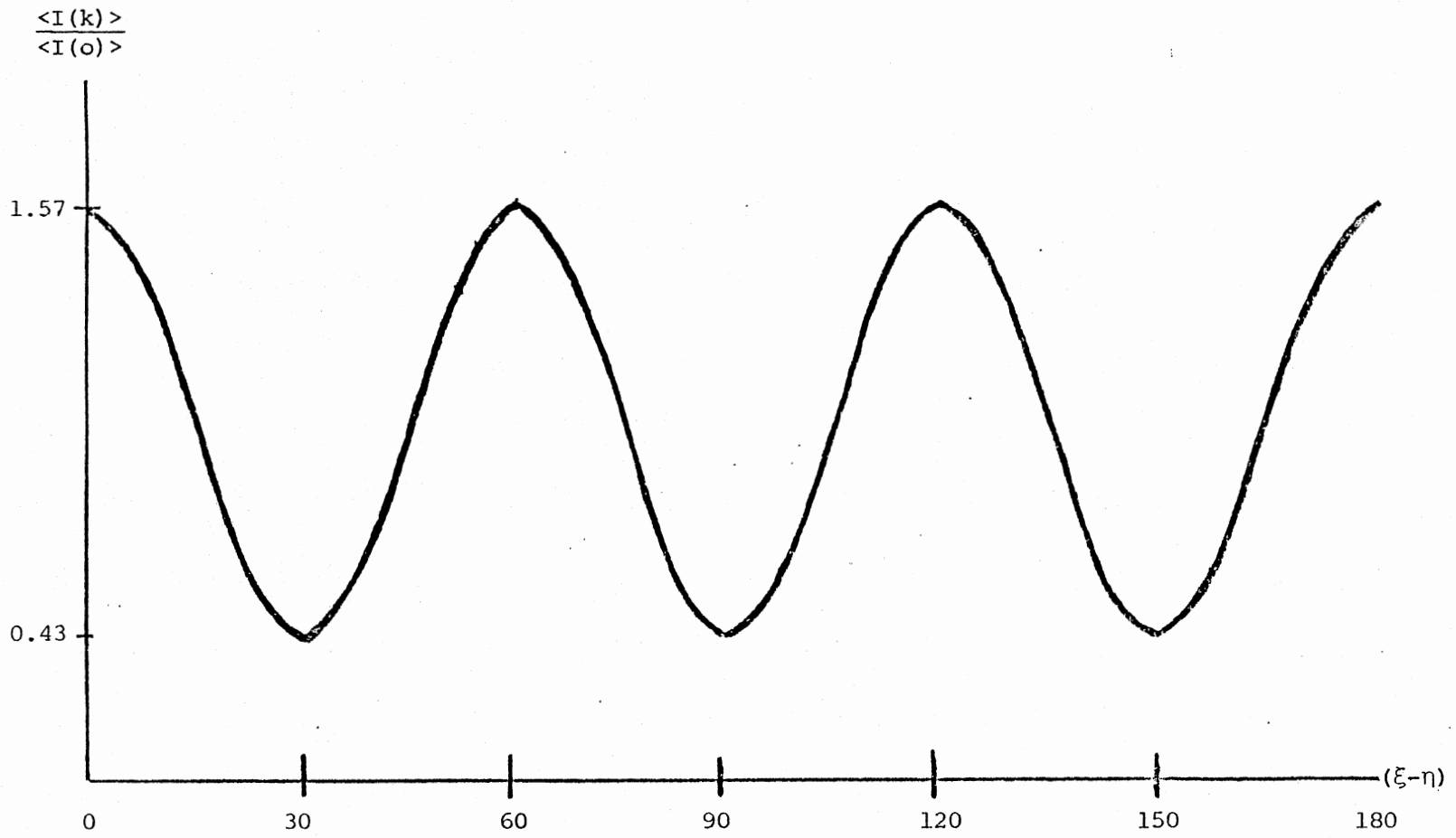

Figure 7. Time-independent Forced Rayleigh Correlation as a Function of the Angle (ξ-η). It Has Maximum Correlation at 0, 60, 120 and Minimum at 30, 90 and 150

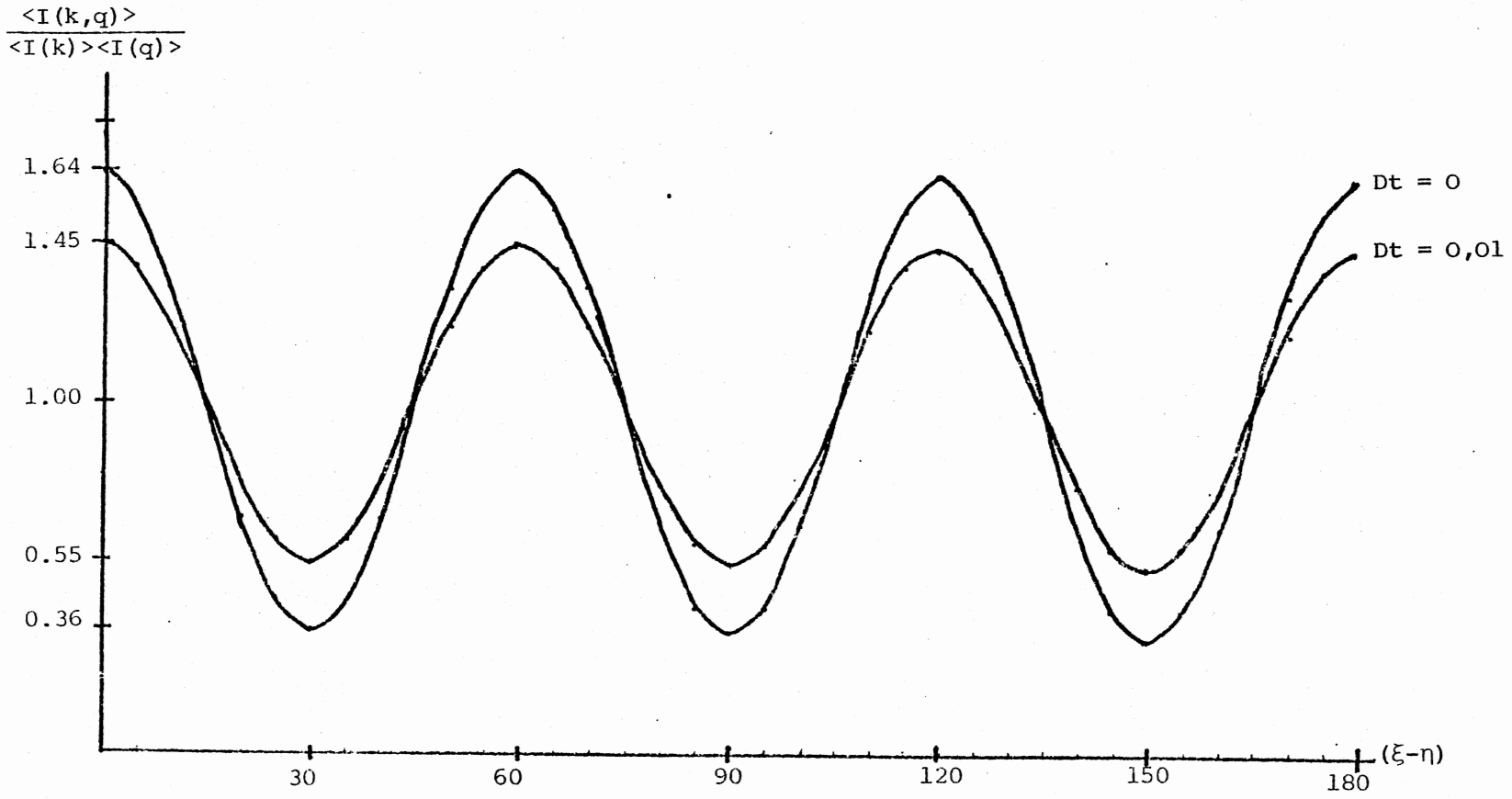

Figure 8. Time-dependent Cross Correlation as a Function of (ξ-η) and Decay Time t. This Figure Shows Correlation and Anti-Correlation Vs. Angle at Different Times. The Lattice Constant is 1.2 um and the Lattice Structure is Hexagonal Close-Packed

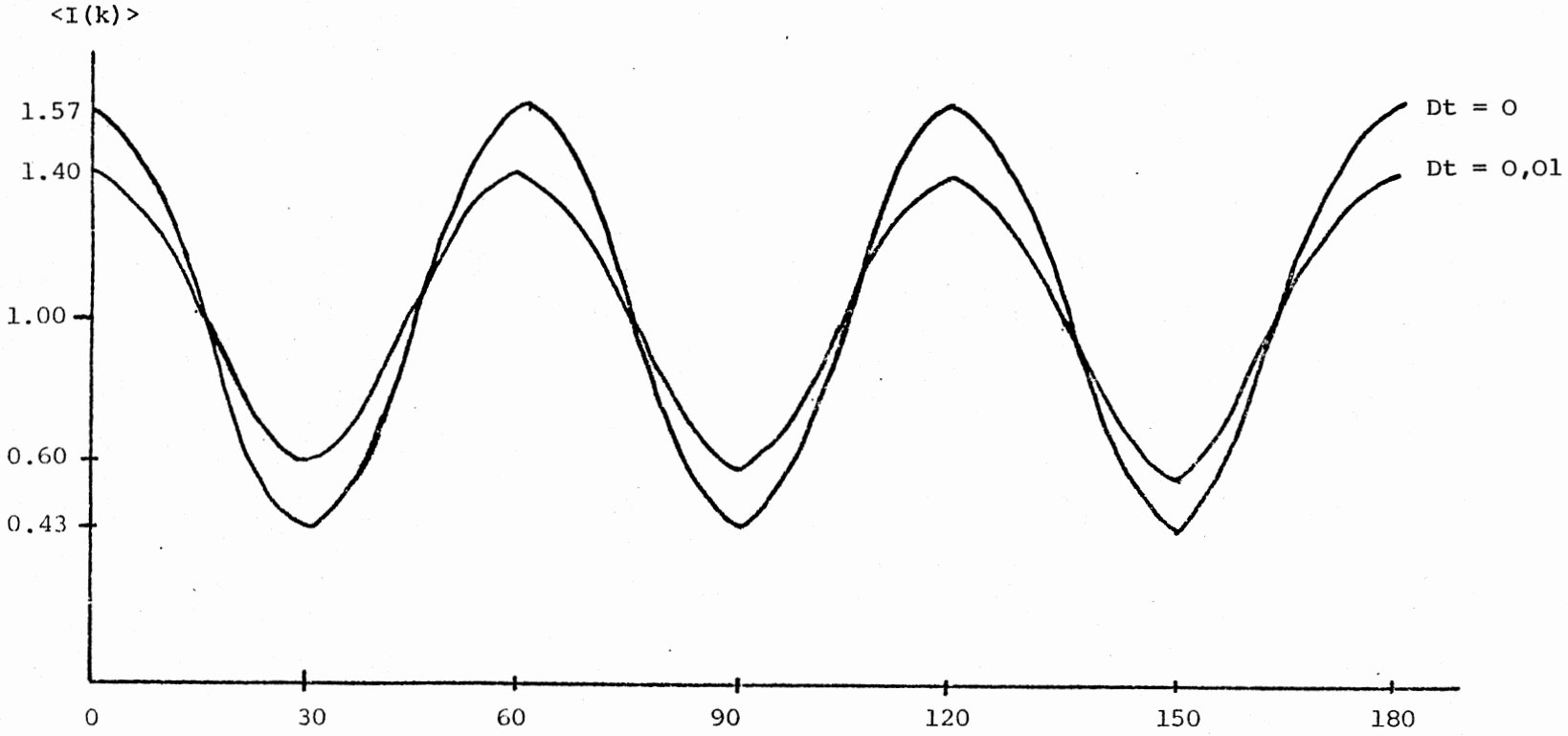

Figure 9. Time-dependent Forced Rayleigh Correlation as a Function of (ξ-η) and Decay Time t. This Figure Shows the Correlation and Anti-Correlation With the Angles at Different Times. It Has Smaller Amplitudes Compared to Cross Correlation Scattering

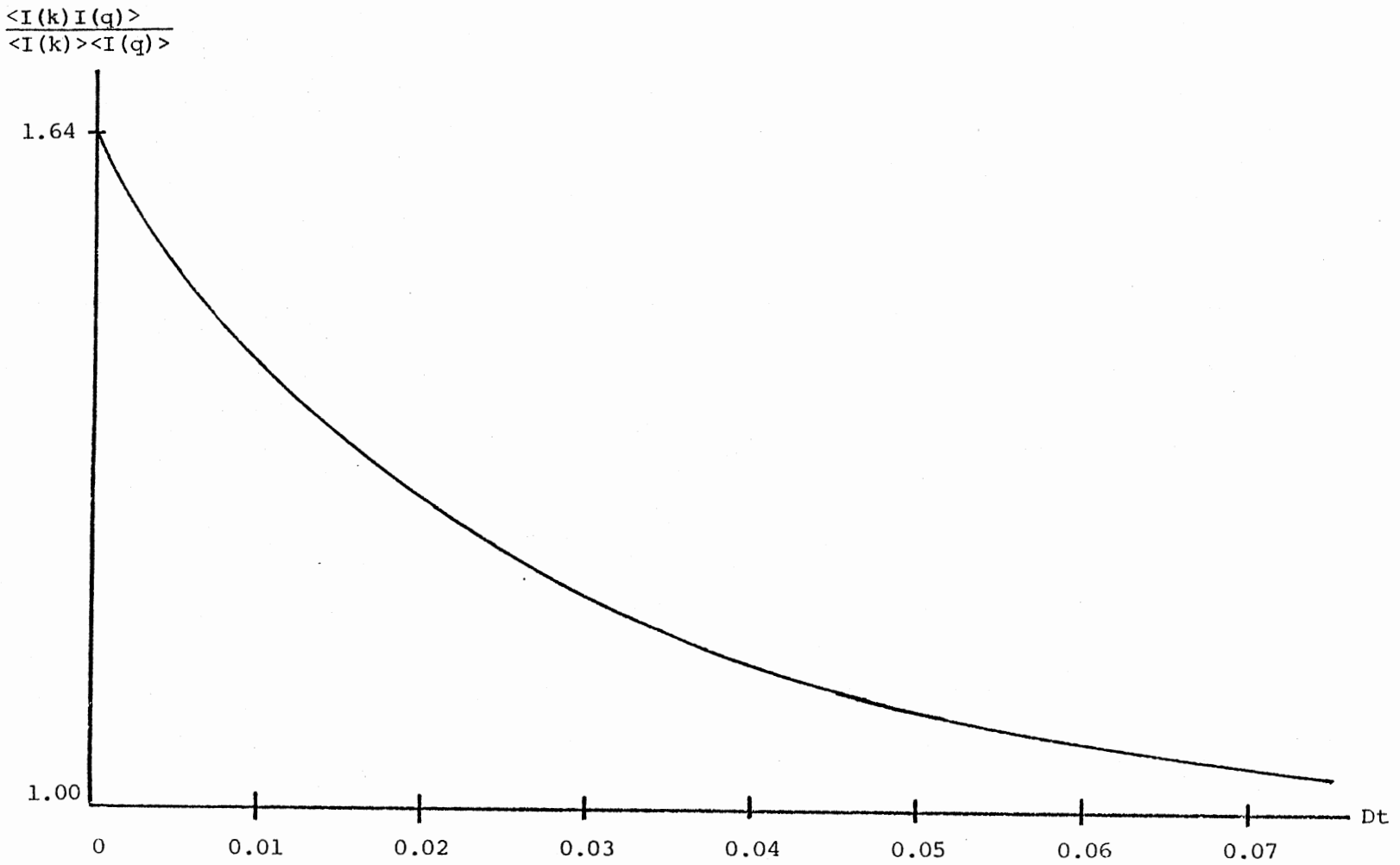

Figure 10. The Decay of Cross Correlation With Fixed $(\xi-\eta) = 0^{o}$. It Shows That the Cross Correlation Decays With Time Monotonically. As Time Increases to Infinity, It Goes to One as the Particles Become Uncorrelated

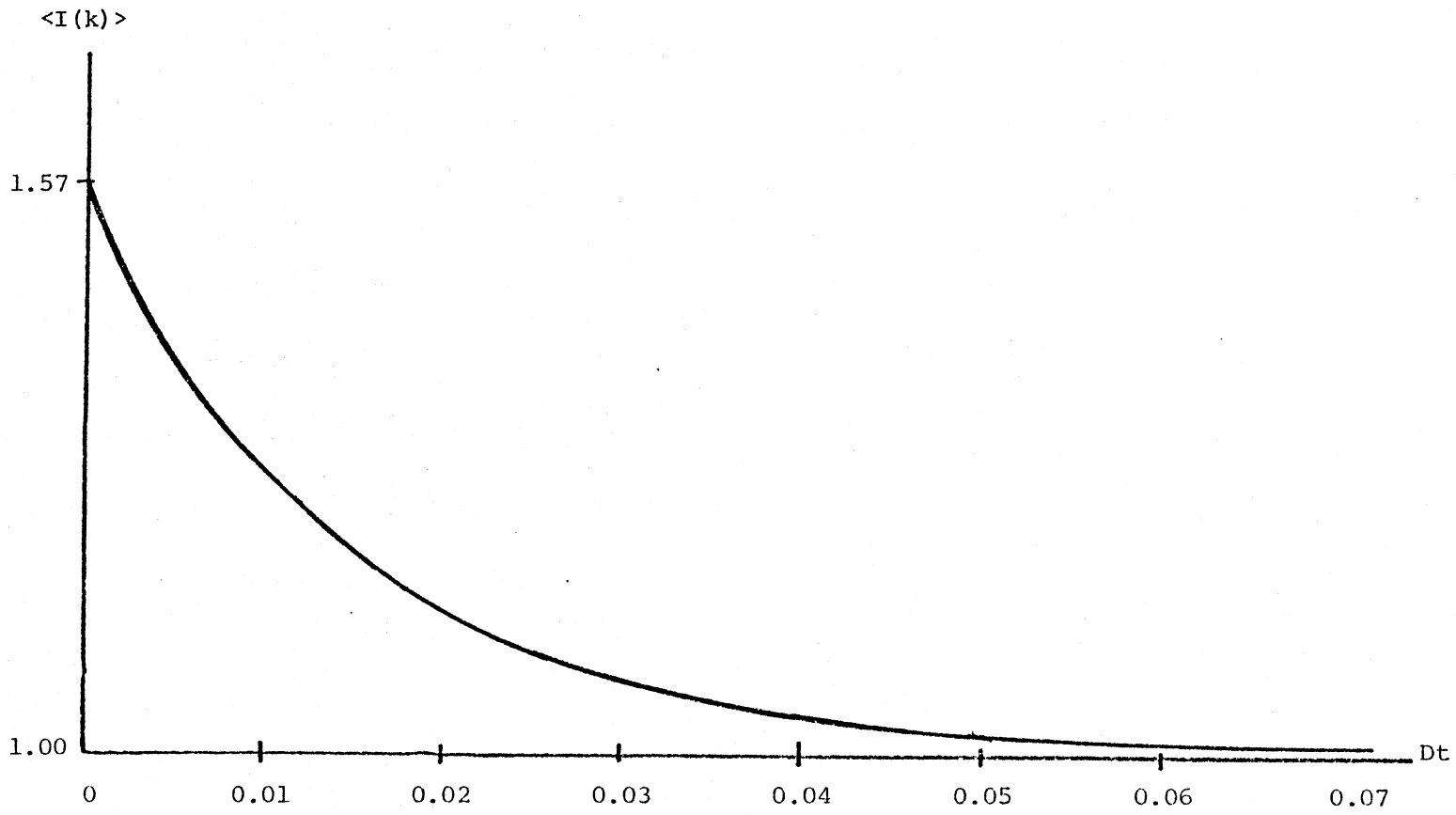

Figure 11. The Decay of Forced Rayleigh Correlation With Fixed $(\xi-\eta) = 0^{o}$. It Shows That the Correlation of Forced Rayleigh Scattering Decays With Time Monotonically.

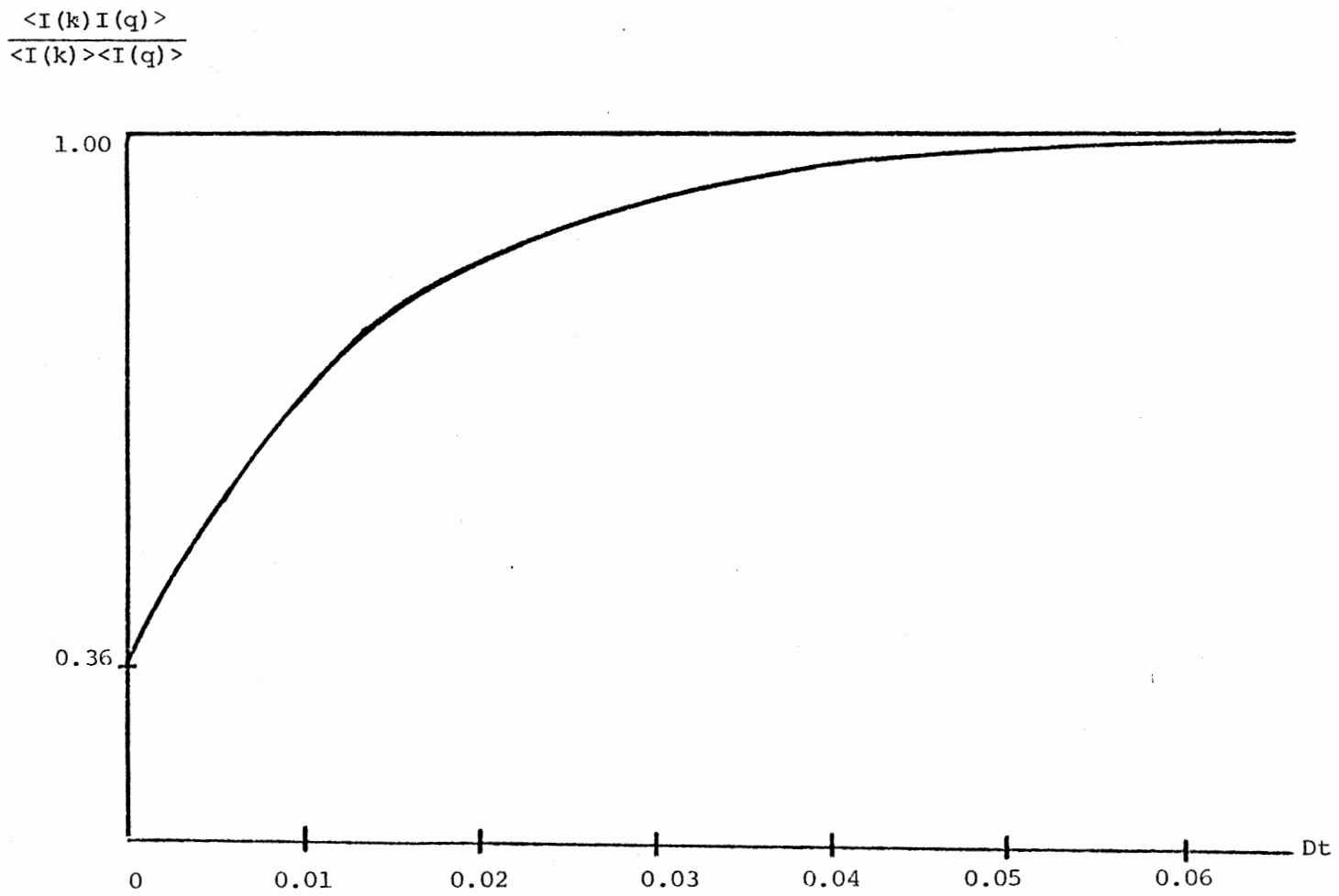

Figure 12. The Decay of Anti-Cross-Correlation With Fixed $(\xi-\eta) = 30^{\circ}$. This Figure Shows That the Anti-Correlation Increases as Time Grows. It Goes to the Value One as Time Increases to Infinity

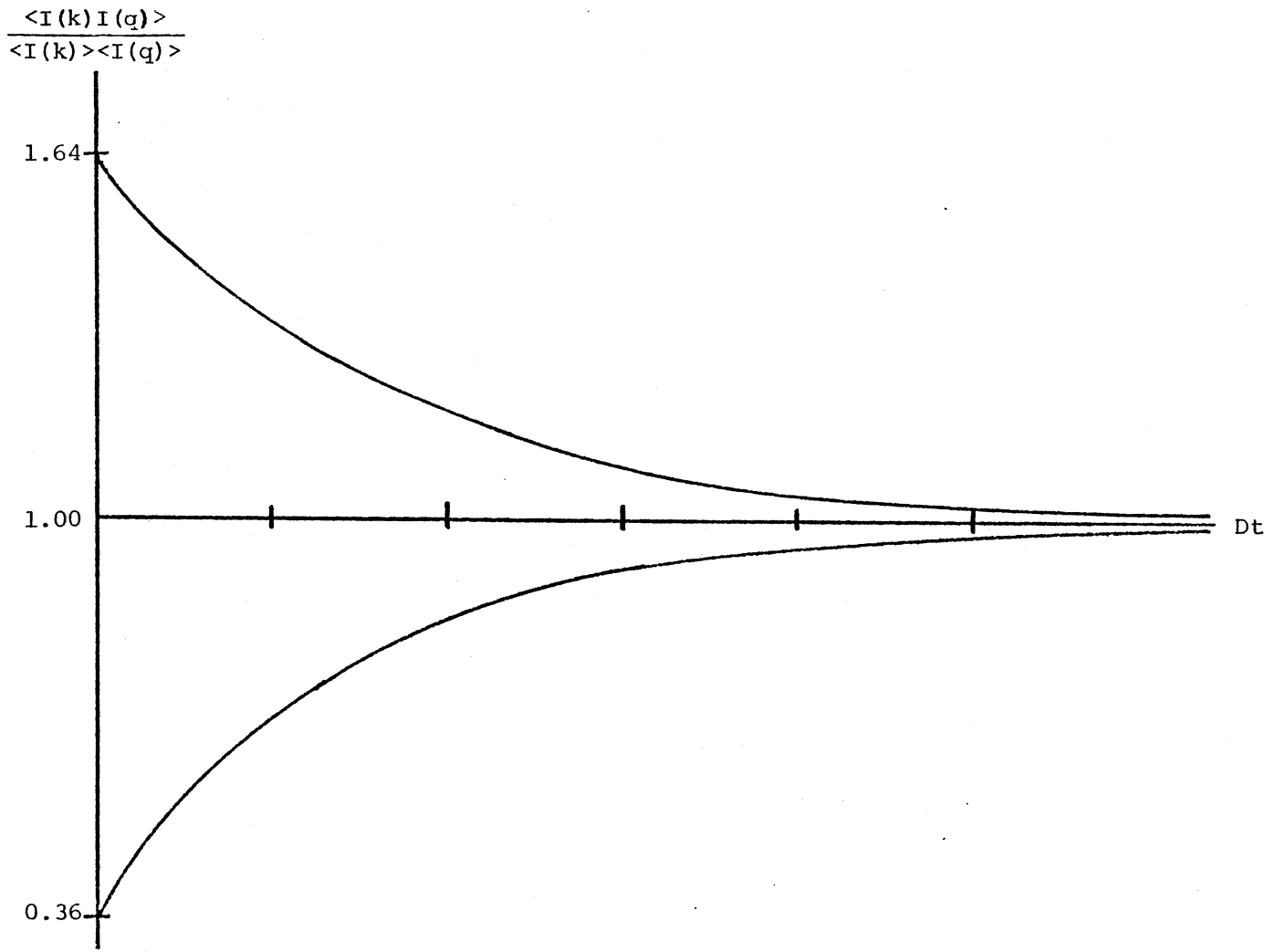

Figure 13. A Comparison Between the Decay of the Cross Correlation at $\eta-\xi = 0^{o}$ and the Decay of the Anti-Cross-Correlation at $\eta-\xi = 30^{o}$

REFERENCES

(1) Pathria, R. K. "Statistical Mechanics", Pergamon Press, New York, 1972.

(2) Eyring, Henry and Mu Shik Jhon. "Significant Liquid Structures", Wiley, New York, 1969.

(3) March, N. H. "Liquid Metals", Pergamon Press, New York, 1968.

(4) Cole, G. H. A. "An Introduction to the Statistical Theory of Classical Simple Dense Fluids", Pergamon Press, New York, 1967.

(5) Fisher, I. Z. "Statistical Theory of Liquids", University of Chicago Press, Chicago, 1964.

(6) Egelstaff, P. A. "An Introduction to the Liquid State", Academic Press, New York, 1967.

(7) Hansen and McDonald. "Theory of Simple Liquids", Academic Press, New York, 1976.

(8) Prins, J. A. and H. Petersen. "Theoretical Diffraction Pattern Corresponding to Some Simple Types of Molecular Arrangement in Liquids", Physica 3, 147 (1936).

(9) Stillinger and A. Weber. Physical Review A 25, 978 (1982).

(10) Ackerson, B. J. "Lectures for master student thesis" (unpublished).

(11) Crosignani, B., P. D. Porto and M. Bertolotti. "Statistical Properties of Scattered Light", Academic Press, New York, 1975.

(12) Watson, G. N. "A Treatise on the Theory of Bessel Function", The Macmillan Company, New York, 1944.

(13) Arfken, G. B. "Mathematical Methods for Physicists", Academic Press, New York, 1970.

(14) Stegun, I. A., M. Abramowitz, MTAC-11, 255-257 (1957).

(15) Abramowitz, M. and I. A. Stegun. "Handbook of Mathematical Function" (Dover, New York, 1965).

(16) Zernike, F. and J. A. Prins, Z. F. Phys. 41, 184 (1937).

(17) Kittel, C. "Introduction to Solid State Physics" (Wiley, New York, 1970).

(18) Pieranski, P. "Two Dimensions Interfacial Colloidal Crystals", Physical Review Letters 45, 569 (1980).

(19) Pieranski, P., L. Strezeleck and J. Friedel. "Observation of Edge Dislocations in Ordered Latexes", Journal de Physique 853 (1979).

(20) Mermin, N. D. "Crystalline Order in Two Dimensions", Physical Review 176, 250 (1968).

(21) Yvon, "Correlations and Entropy in Classical Statistical Mechanics", Pergamon Press, New York, 1969.

(22) Imry, Y. "Long Range Order in Two Dimensions" CRC Critical Reviews in Solid State and Material Science 157 (1979).

(23) Ashcroft, N. W. and N. D. Mermin, "Solid State Physics" (Holt, New York, 1976).

(24) Smith, P. W., A. Ashkin and W. J. Tomlinson, "Four-Wave Mixing in an Artificial Kerr Medium", Optics Letters 6, 6 (1981).

APPENDIX A

PROGRAM FOR BESSEL'S FUNCTION CALCULATION

This program is used to calculate the Bessel's function values. It is good for any order and argument.

```
LIST

CCHEN     MU BASIC/RT-11 VOL-01C

10 REM BESSEL FUNCTION
11 DIM 1(50);T(100)
15 PRINT "N";"X";"1(X)"
20 FOR L=0 TO 50
30 FOR A3=0 TO 50 STEP 5
40 IF A3=0 THEN 900
42 F9=7:97885*100(-1)-7:7*100(-7)*(3/A3)-5:5274*100(-3)*(3/A3)92
43 F8=-9:512*100(-5)*(3/A3)93+1:37237*100(-3)*(3/A3)94
44 F7=-7:2805*100(-4)*(3/A3)25+1:4476*100(-4)*(3/A3)96
45 F0=F9+F8+F7-4:4*100(-7)
46 G9=A3-7:854*100(-1)
47 G8=-4:1664*100(-2)*(3/A3)-3:954*100(-5)*(3/A3)92
48 G7=2:6257*100(-3)*(3/A3)93-5:4125*100(-4)*(3/A3)94
49 G6=-2:9333*100(-4)*(3/A3)95+1:3558*100(-4)*(3/A3)96
50 G0=G9+G8+G7+G6+1:84*100(-5)+3*100(-8)*(3/A3)+3*100(-8)*(3/A3)93
51 F6=7:9788*100(-1)+1:56*100(-6)*(3/A3)
52 F5=1:6597*100(-2)*(3/A3)92+1:7105*100(-4)*(3/A3)93
53 F4=-2:4951*100(-3)*(3/A3)94+1:1365*100(-3)*(3/A3)95
54 F3=-2:0033*100(-4)*(3/A3)96
55 F1=F6+F5+F4+F3+4:56*100(-6)-3:3*100(-7)*(3/A3)*1022-100(-8)*(3/A3)*10
54
56 G5=A3-2:3562+1:2499*100(-1)*(3/A3)
57 G4=5:65*100(-5)*(3/A3)92-6:3788*100(-3)*(3/A3)93
58 G3=7:4348*100(-4)*(3/A3)94+7:9824*100(-4)*(3/A3)95
59 G2=-2:9166*100(-4)*(3/A3)96
60 G1=G5+G4+G3+G2+5:51*100(-6)+6:12*100(-6)*(3/A3)+100(-8)*(3/A3)*1003
61 1(0)=A39(-:5)*F0*C09(G0)
62 1(1)=A39(-:5)*F1*C09(G1)
90 IF L>A3 THEN 96
92 FOR K=2 TO L
93 1(K)=2*(K-1)/A3*1(K-1)-1(K-2)
94 NEXT K
95 GO TO 888
96 GOSUB 1000
97 1(L)=1(L)/10010
888 PRINT L:A3:1(L)
900 NEXT A3
950 NEXT L
999 END
1000 REM-SUBROUTINE-
1010 D=20
1020 F=L+D
1030 T(F)=0
1040 T(F-1)=100(-30)
1050 FOR H=2 TO F
1060 T(F-H)=(2*(F-H+1)/A3)*T(F-H+1)-T(F-H+2)
1070 NEXT H
1080 S1=T(0)
1090 FOR I=2 TO F STEP 2
```

```
1100 S1=S1+2*T(I)
1110 NEXT I
1120 D9=10010/S1
1130 1(L)=D9*T(L)
1140 RETURN
```

APPENDIX B

PROGRAM FOR CORRELATION FUNCTION CALCULATION

This program is used to calculate the cross correlation function.

```
CYCHEN      MU BASIC/RT-11 VOL-01C


1 DIM V1(5:5):V2(5:5):D(50):E(50)
2 DIM J(50):T(150):R9(50):19(50):B(50):C(50)
3 Z=(37:51/180)*PI
4 Z1=SIN(Z)
5 A=1:2*100(-6)
6 A1=:5*A
7 A2=(39:5/2)*A
8 FOR M=-1 TO 1
9 FOR N=-1 TO 1
10 V1(M+2:N+2)=(M-2*N)*A1
11 V2(M+2:N+2)=M*A2
12 NEXT N
13 NEXT M
14 FOR L=O TO 6
15 B(L)=O
16 C(L)=O
17 FOR M=-1 TO 1
18 FOR N=-1 TO 1
19 FOR P=-1 TO 1
20 FOR Q=-1 TO 1
21 IF M=1 THEN IF N=-1 THEN 800
22 IF P=1 THEN IF Q=-1 THEN 800
23 IF M=-1 THEN IF N=1 THEN 800
24 IF P=-1 THEN IF Q=1 THEN 800
25 IF M=-2 THEN IF N=1 THEN 800
26 IF M=-2 THEN IF N=2 THEN 800
27 IF P=2 THEN IF Q=-2 THEN 800
28 IF P=2 THEN IF Q=-1 THEN 800
29 IF P=1 THEN IF Q=-2 THEN 800
30 IF P=-1 THEN IF Q=2 THEN 800
31 IF P=-2 THEN IF Q=1 THEN 800
32 IF P=-2 THEN IF Q=2 THEN 800
33 V=V1(P+2:Q+2)-V1(M+2:N+2)
34 U=V2(P+2:Q+2)-V2(M+2:N+2)
35 D5=(V92+U92)9:5
36 IF D5=O THEN IF L=O THEN 65
37 IF D5=O THEN IF L>O THEN 800
38 A3=D5*2*PI*1:59/(:6328*100-6)*Z1
42 F9=7:97885*100(-1)-7:7*100(-7)*(3/A3)-5:5274*100(-3)*(3/A3)92
44 F7=-7:2805*100(-4)*(3/A3)95+1:4476*100(-4)*(3/A3)96
45 FO=F9+F8+F7-4:4*100(-7)
46 G9=A3-7:854*100(-1)
47 G8=-4:1664*100(-2)*(3/A3)-3:954*100(-5)*(3/A3)92
48 G7=2:6257*100(-3)*(3/A3)93-5:4125*100(-4)*(3/A3)94
49 G6=-2:9333*100(-4)*(3/A3)95+1:3558*100(-4)*(3/A3)96
50 GO=G9+G8+G7+G6+1:84*100(-5)+3*100*-8)*(3/A3)+3*100(-8)*(3/A3)93
51 F6=7:9788*100(-1)+1:56*100(-6)*(3/A3)
52 F5=1:6597*100(-2)*(3/A3)92+1:7105*100(-4)*(3/A3)93
53 F4=-2:4951*100(-3)*(3/A3)94+1:1365*100(-3)*(3/A3)95
54 F3=-2:0033*100(-4)*(3/A3)96
```

```
55 F1=F6+F5+F4+F3+4:56*100(-6)-3:3*100(-7)*(3/A3)*1002-100(-8)*(3/A3)*10
24
56 G5=A3-2:3562+1:2499*100(-1)*(3/A3)
57 G4=5:65*100(-5)*(3/A3)92-6:3788*100(-3)*(3/A3)93
58 G3=7:4348*100(-4)*(3/A3)94+7:9824*100(-4)*(3/A3)95
59 G2=-2:9166*100(-4)*(3/A3)96
60 G1=G5+G4+G3+G2+5:51*100(-6)+6:12*100(-6)*(3/A3)+100(-8)*(3/A3)*1003
61 J(O)=A30(-:5)*FO*COS(GO)
62 J(1)=A30(-:5)*F1*COS(G1)
65 C1=V1(P+2:Q+2)92+V2(P+2:Q+2)92
66 C2=V1(M+2:N+2)92+V2(M+2:N+2)92
67 C=(C1+C2)*10012
68 E=EXP(-C)
69 IF D5=O THEN IF L=O THEN 71
70 GO TO 88
71 L1=O
72 G1=O
73 J(O)=1
74 GO TO 400
88 IF L=O THEN 98
89 IF L=1 THEN 98
90 IF L>A3 THEN 96
91 IF L>1 THEN 92
92 FOR K=2 TO L
93 J(K)=2*(K-1)/A3*J(K-1)-J(K-2)
94 NEXT K
95 GO TO 98
96 GOSUB 1000
97 J(L)=J(L)/10210
98 T8=4
99 FOR W=O TO 15
100 T9=T8*W
101 L1=L-T9
102 IF L1<4 THEN 110
103 NEXT W
110 D7=ABS(V1(P+2:Q+2)-V1(M+2:N+2))
111 D8=ABS(V2(P+2:Q+2)-V2(M+2:N+2))
120 IF V1(P+2:Q+2)<V1(M+2:N+2) THEN IF V2(P+2:Q+2)=V2(M+2:N+2) THEN 130
125 GO TO 150
130 Q1=PI/2
140 GO TO 400
150 IF V1(P+2:Q+2)<=V1(M+2:N+2) THEN IF V2(P+2:Q+2)>V2(M+2:N+2) THEN 170
160 GO TO 190
170 Q1=PI-ATN(D7/D8)
180 GO TO 400
190 IF V1(P+2:Q+2)<=V1(M+2:N+2) THEN IF V2(P+2:Q+2)<V2(M+2:N+2) THEN 210
200 GO TO 230
210 01=ATN(D7/D8)
220 GO TO 400
230 IF V1(P+2:Q+2)>V1(M+2:N+2) THEN IF V2(P+2:Q+2)=V2(M+2:N+2) THEN 250
240 GO TO 270
250 G1=-PI/2
260 GO TO 400
```

```
270 IF V1(P+2:Q+2)>=V1(M+2:N+2) THEN IF V2(M+2:N+2)<V2(P+2:Q+2) THEN 290
280 GO TO 310
290 Q1=-(PI-ATN(D7/D8))
300 GO TO 400
310 IF V1(P+2:Q+2)>=V1(M+2:N+2) THEN IF V2(M+2:N+2)>V2(P+2:Q+Z) THEN 330
330 Q1=-ATN(D7/D8)
400 IF V1(M+2:N+2)=O THEN IF V2(M+2:N+2)>=O THEN 402
401 GO TO 404
402 GO=O
403 GO TO 750
404 GO=PI
405 GO TO 750
406 IF V1(M+2:N+2)<O THEN IF V2(M+2:N+2)=O THEN 413
407 IF V2(M+2:N+2)>O THEN 409
408 GO TO 411
409 GO=ATN(ABS(V1(M+2:N+2))/V2(M+2:N+2))
410 GO TO 750
411 GO=PI-ATN(V1(M+2:N+2)/V2(M+2:N+2))
412 GO TO 750
413 GO=PI/2
414 GO TO 750
415 IF V1(M+2:N+2)>O THEN IF V2(M+2:N+2)=O THEN 422
416 IF V2(M+2:N+2)>O THEN 418
418 GO=-ATN(V1(M+2:N+2)/V2(M+2:N+2))
419 GO TO 750
420 GO=-(PI-ATN(V1(M+2:N+2)/ABS(V2(M+2:N+2))))
421 GO TO 750
422 GO=-PI/2
423 GO TO 750
750 P1=COS(L*(Q1-QO))
751 P2=SIN(L*(Q1-QO))
753 P3=COS(L*GO)
754 P4=-SIN(L*GO)
758 IF L1=O THEN 762
760 GO TO 766
762 R9(L)=J(L)*P1
764 I9(L)=J(L)*P2
765 GO TO 791
766 IF L1=1 THEN 770
768 GO TO 776
770 R9(L)=-J(L)*P2
772 I9(L)=J(L)*P1
774 GO TO 791
776 IF L1=2 THEN 780
778 GO TO 786
780 R9(L)=-J(L)*P1
782 I9(L)=-J(L)*P2
784 GO TO 791
786 IF L1=3 THEN 788
788 R9(L)=J(L)*P2
789 I9(L)=-J(L)*P1
790 IF D5=O THEN 796
791 B(L)=B(L)+:5*R9(L)*E
```

```
792 C(L)=C(L)+:5*I9(L)*E
793 D(L)=D(L)+:5*(R9(L)*E*P3-I9(L)*E*P4)
794 E(L)=E(L)+:5*(I9(L)*E*P3+R9(L)*E*P4)
795 GO TO 800
796 B(L)=B(L)+R9(L)*E
797 C(L)=C(L)+I9(L)*E
798 D(L)=D(L)+R9(L)*E*P3-I9(L)*E*P4
799 E(L)=E(L)+I9(L)*E*P3+R9(L)*E*P4
800 NEXT Q
805 NEXT P
810 NEXT N
815 NEXT M
820 PRINT L:B(L):C(L):D(L):E(L)
825 NEXT L
830 FOR R=O TO 180
831 FOR D8=O TO 50 STEP 10
832 D7=1:00000E-03
835 I1=O
850 J1=O
851 I2=O
852 I3=O
854 FOR S=-6 TO 6
855 A=5
856 IF S>=O THEN 870
867 J1=J1+(B(-S)92+C(-S)92)*COS(S*R*A*PI/180)
868 I1=I1+(B(-S)92+C(-S)92)*COS(S*R*A*PI/180)*EXP(-S92*D7*D8)
869 GO TO 890
870 J1=J1+(B(S)92+C(S)92)*COS(S*R*A*PI/180)
871 I1=I1+(B(S)92+C(S)92)*COS(S*R*A*PI/180)*EXP(-S92*D7*D8)
872 I2=I2+(D(S)*COS(S*R*A*PI/180)-E(S)*SIN(S*R*A*PI/180))
873 I3=I3+(D(S)*COS(S*R*A*PI/180)-E(S)*SIN(S*R*A*PI/180))*EXP(-S92*D7*D8
O
890 NEXT S
895 W9=R*A
913 R3=12/B(O)
914 R4=I3/B(O)
915 R1=I1/(B(O)92+C(O)92)
916 R2=J1/(B(O)92+C(O)92)
917 X1=D7*D8
920 PRINT W9:R2:R1:R3:R4
921 NEXT D8
925 NEXT R
999 END
1000 REM-SUBROUTINE-
1010 D=20
1020 F=L+D
1030 T(F)=O
1040 T(F-1)=109(-30)
1050 FOR H=2 TO F
1060 T(F-H)=(2*(F-H+1)/A3)*T(F-H+1)-T(F-H+2)
1070 NEXT H
1080 S1=T(O)
1090 FOR I=2 TO F STEP 2
```

```
1100 S1=S1+2*T(I)
1110 NEXT I
1120 D9=10010/91
1130 J(L)=D9*T(L)
1140 RETURN

READY
```

VITA

Ching-Yuan Chen

Candidate for the Degree of

Master of Science

Thesis: THEORETICAL STUDY OF CORRELATION IN TWO DIMENSIONAL HCP STRUCTURE

Major Field: Physics

Biographical:

Personal Data: Born in Tainan, Taiwan, R.O.C., 1 March, 1950, the son of Mr. and Mrs. Y. C. Chen.

Education: Graduated from Tainan First High School in June, 1969; received Bachelor of Science degree in Applied Mathematics in 1973 from National Taiwan Chung Hsing University; served in the army in Taiwan from 1973 to 1975; a graduate student in the Department of Physics of National Taiwan University between 1977-1978 and graduate study in the University of Arkansas, Fayetteville, Arkansas, in the Spring of 1979; completed requirements for the Master of Science degree at Oklahoma State University in July, 1982.